THE PLATEAU-RAYLEIGH INSTABILITY: AN INVESTIGATION OF FALLING FLUID JETS

THOMAS VAN MANEN

1. Introduction

A fluid jet emanating from a circular, downward-pointing nozzle does not continue moving within a cylindrically confined space after leaving the nozzles head. Rather, the jets shape is perturbed from the expected cylinder and becomes unstable, increasing with distance from the head; and, below a certain height, the jet breaks up into discrete spherical droplets. This phenomenon, called the Plateau-Rayleigh (PR) instability, is essentially that of the dripping tap readily provided for observation in any household setting, yet the physics and mathematics of its description are of surprising consequence.

In many scenarios the dominating force in falling jet dynamics is surface tension. In such cases, the physical description of jet shape reduces to a mathematical minimization of jet surface area. Similar minimization problems arise in other areas of physics. In fact, Plateaus motivation in studying fluids in the 1800s was to shed light on the forces cohering galaxies.[2] More recently, Cardoso[3] and others have suggested that drawing analogy between fluid phenomena and predicted n-dimensional gravitational phenomena may help inform intuitions about the latter (treating entropy maximization in the latter as analogous to surface minimization in the former).[3] Cardoso claims that in this manner, study of the PR instability will give insight to the conditions for stability of black strings in n-dimensional spacetime. Understanding the jet break-up conditions in the fluid case may help predict the collapse conditions of higher-dimensional black objects into observable black holes.

While experimental confirmation of n-theories would be cool, it is perhaps less feasible than the other applications of PR instability analysis, which are manifold. Simple nozzles are used in all manner of industry; from lubricating and coating manufactured components, to bottling water and other liquids. The PR instability is of central importance in ink-jet printer nozzle design. The above applications involve a wide range of fluids, so naturally an understanding of the physics over a similar range is desired. The purpose of this experiment is to determine the limitations of the

inviscid assumption used to develop the theoretical model of the Plateau-Rayleigh instability.

1.1. **Dimensional analysis.** The following derivations of the physical theory behind the Plateau-Rayleigh instability are modelled off of the lecture notes of T R Akylas [8]. First, a non-dimensional equation for jet speed is derived from the Bernoulli relation coupled with the Young-Laplace equation. In order to equate the Bernoulli function at two points in the jet, inviscid (high Reynolds number) flow must be assumed. If z is taken to be the vertical scale, then (assuming constant density and irrotational flow as well),

$$B \equiv \frac{q_A^2}{2} + P_A + gz_A = \frac{q_B^2}{2} + P_B + gz_B \tag{1}$$

for any two points A and B in the flow, where $q^2/2$, P and z are the kinetic energy, pressure and height at those points. Meanwhile the Young-Laplace equation relates the change in pressure ΔP across a fluid-air interface to the curvature $\nabla \cdot \hat{n}$ of the interface according to

$$\Delta P = \sigma(\nabla \cdot \hat{n}) \tag{2}$$

where σ is the surface tension of the fluid. The mean curvature at height z can be approximated as

$$\nabla \cdot \hat{n} \approx \frac{1}{r}$$

where r is the jet radius at z. Then setting point A just inside the nozzle, $z = 0$ at the base of the jet and substituting (2) into (1),

$$\frac{\rho U_0^2}{2} + \frac{\sigma}{a} + gz = \frac{\rho U(z)^2}{2} + \frac{\sigma}{r}$$

Scaling speed by U_0, distance by a, and solving for $U(z)$,

$$\frac{U(z)}{U_0} = \left(1 + \frac{2}{Fr}\frac{z}{a} + \frac{2}{We}\left(1 - \frac{a}{r}\right)\right)^{1/2} \tag{3}$$

Here, nondimensional numbers of Weber and Froude have been introduced:

$$We \equiv \frac{\rho U_0^2 a}{\sigma},$$

$$Fr \equiv \frac{U_0^2}{ga}$$

The Weber number relates the inertia of flow to surface tension, whereas the Froude number relates inertia to gravitational forces. The experiments reported here investigated flow regimes for which $We \gg Fr$, so that (3) was reducible to

$$\frac{U(z)}{U_0} \approx \left(1 + \frac{2}{Fr}\frac{z}{a}\right)^{1/2}, \tag{4}$$

a relation later used to deduce flow speed at the jet's base.

1.2. **Finding a dispersion relation.** Having established a basic understanding of the flow of an ideal jet, the next step is to investigate the formation of the Plateau-Rayleigh instability. The investigation begins by considering a smooth, vertically-oriented cylindrical jet of initial radius R_0 (z-uniform). Then, a small axisymmetric perturbation $R = \hat{R}e^{\omega t + ikz}$ is introduced to the surface of the jet, so that its radius becomes

$$R_0 + \hat{R}e^{\omega t + ikz}$$

where k is the (real) wavenumber of the perturbation and ω is its (in general complex) decay constant. The speed is expected to vary similarly, so that by substituting the perturbation into the equations of motion, a dispersion relation can be derived. Akylas [8] proceeds to show that the vertical and radial momentum equations and the continuity equation, combined with two boundary conditions, produce the following dispersion relation:

$$\omega^2 = \frac{\sigma}{\rho R_0^3} kR_0 \frac{I_1(kR_0)}{I_0(kR_0)}(1 - (kR_0)^2) \tag{5}$$

(One condition equated the rate of change of radius with the radial component of jet velocity at the jet's surface, as required by continuity. The other boundary condition was derived from the Young-Laplace equation (2) and related the initial (unperturbed) pressure and radius of the jet.) In (5), ρ represents fluid density, and the functions I_0 and I_1 are the zeroth and first order modified Type II Bessel polynomials.

In practice, standing waves are much easier to observe than a perturbed jet with unstable features. Standing waves form when a jet impinges upon a reservoir rather than falling to the height at which droplet formation would otherwise occur. In this situation, the perturbations that normally induce jet break-up are instead reflected by the surface of the reservoir and travel back upward along the jet. The frequency of perturbation which propagates at speed equal and opposite to that of the falling jet, satisfying

$$\frac{|\omega|}{k} = -U_{jet}$$

forms a wave that appears stationary in the lab frame. Recall that the decay constant ω of the perturbation is generally complex, and in the case of standing waves, ω is purely imaginary, representing a travelling wave with angular frequency $|\omega|$. According to (5) then,

$$U_{jet}^2 = \frac{|\omega|^2}{k^2} = \frac{-\sigma}{\rho k R_0^2} \frac{I_1(kR_0)}{I_0(kR_0)}(1 - (kR_0)^2) \tag{6}$$

Thus by measuring the wavelength of a standing wave, the dispersion relation can be used to predict the jet's speed as it impinges on a reservoir, which by comparison to other speed measurements provides an opportunity to test the validity of the dispersion relation.

2. Procedure

2.1. **Apparatus.** A large beaker of fluid was positioned above the main apparatus, and from it fluid was siphoned via nalgene tubing, through a spigot and into a bottle with a nozzle protruding from its base. The bottle was clamped to a lab stand and held above a tray which sat upon a digital mass scale. A digital webcam recorded the shape of the fluid jet over intervals of $\sim 15s$. Before each recording period, the height of the nozzle above the sink reservoir was adjusted to produce a clear standing wave. Then data acquisition was initiated using webcam software, and time and sink reservoir mass were recorded at the beginning and end of the interval to determine mean flow rate from the nozzle. Graphical Analysis was used to measure wavelength, jet radius and nozzle height in several sample frames of each video clip to obtain mean values, with which (6) predicted jet speed U_{jet} at the sink interface. Jet radius was smaller than the other dimensions measured, so to minimize measurement uncertainty, a mean of five radius measurements was taken from each sample frame. This was then used as an estimate of R_0, the unperturbed jet radius. Also, in calculating U_{jet} from (5), only the first three terms in the Bessel polynomials were retained. It was found that within the range of measured k and R_0, higher order terms quickly approached zero (converging as $1/n!$), so that this approximation did not noticeably affect the accuracy of dispersion relation predictions. U_{jet} was also determined directly by employing (4) and a reasonable density estimate (see section 2.2).

During each data acquisition period, it was essential to maintain time-uniform laminar flow through the nozzle, both to ensure the accuracy of mean flow rate measurements and to establish a stable standing wave. The presence of the bottle as an intermediary chamber between the source reservoir and the nozzle aided in both respects. Whereas the column height (and driving pressure) in the source reservoir

dropped over time, a constant fluid column height could be maintained in the intermediary chamber. Additionally, this mechanism allowed for the fluid column height to be decreased significantly (to $\sim 5mm$) to produce a very low driving pressure above the nozzle and the desired laminar outflow. The mass measurements used to determine flow rate were also subject to error due to flow non-uniformity, in the sense that the jet's impact on the sink reservoir had a noticeable effect on the mass measured by the scale. Thus all mass measurements were taken in the presence of the jet, and its mean impact pressure ($\propto U_{jet}$) was assumed constant.

2.2. **Materials.** The experiment was performed with a range of sugar solutions with the intention of observing the effect of viscosity on fluid jet shape. A stock solution of $\sim$ 70% sucrose was prepared, from which subsequent dilutions were produced. The solution concentrations and corresponding fluid properties are given in the table below.

Sucrose ($wt\%$)	Density (g/cm^3)	Viscosity ($g/cm \cdot s$)	Surface Tension (g/s^2)
0%	0.9968	10.1	72.8
9.4%	1.0338	13.4	73
27%	1.1118	27	74
50.1%	1.2324	170	76
53.6%	1.2511	250	76
66.8%	1.3267	2100	79
70.4%	1.3498	5400	79

Sucrose concentrations were measured prior to each experiment using a handheld refractometer. (For high concentration solutions, samples were diluted in water before the refractometer was used.) Density and viscosity were estimated based on concentration using Flanagan's methods, available here [5]. Surface tension was estimated by using a third order polynomial interpolation of known surface tension data relating σ to sucrose concentration (see Figure 3).

3. Results and Discussion

Two methods of determining U_{jet} are compared in Figure 4, showing a clear linear relationship between the measured and predicted values for low to midrange (0%-50%) concentration sucrose solutions. For higher concentrations, measured U_{jet} values lie well below the baseline set by low concentrations, reflecting an overestimate of U_{jet} by (6). Qualitatively at least, this is a reasonable result because the derivation of the dispersion relation assumed inviscid flow, modelling a faster, less impeded jet than the observed one. Furthermore, the drastic increase in baseline deviation with

concentration (as seen from 50.1% to 53.6%) reflects an exponential dependence on concentration similar to that of viscosity and unlike the power-like relations of density or surface tension.

Although the linear trend for low viscosity jets is well-pronounced, its non-unit slope and non-zero intercept are of some concern (since the theory claims that identical values are being compared). While the size of uncertainties depicted in Figure 4 appear to allow for a linear baseline much closer to the identity line, the chosen baseline is believed to be correct because it correlates well with almost all measured values, and the outlying data points are easily explained.

The size of vertical error bars in Figure 4 was largely determined by the uncertainty in measured mass flux, which was quite large because mass differences of $\sim$ 10g had to be measured over a background mass of $\sim$ 500g imposed by the sink reservoir's weight. Meanwhile, the main contributor to the size of horizontal error bars was the set of surface tension values estimated according to Figure 3. The surface tension estimate is likely the main cause of deviation of baseline slope from unity. It is not the only significant contributor however, because even the experimental trials of water (0%), a fluid with well-known surface tension, had a rather poor correlation between U_{exp} and U_{th}.

The single data point for 10.1% sucrose solution, the first data point recorded in the lab, had a surprising U_{exp}:U_{th} correlation of 1.01:1, which suggests alternatively that the odd correlation may simply be an artefact of the experimental setup used in the lab.

4. Conclusions

These experiments provide strong evidence that the dispersion relation derived for the inviscid Plateau-Rayleigh instability is applicable to viscosities of up to the order of $170 g/cm \cdot s$. Furthermore, they show that observation of a standing wave produced by the Plateau-Rayleigh instability may be used to determine the rate of flow from a nozzle.

5. Acknowledgments

References

[1] Lord Rayleigh, *On the capillary phenomenon of jets.* Proc. Roy. Soc. Lon., v.29 pp71-97, 1879.
[2] Joseph Plateau, *Statique experimentale et theorique des liquides soumis aux seules forces moleculaires.* 1973.

[3] Vitor Cardoso, *The return of the membrane paradigm? Black holes and strings in the water tap*. 2008.
[4] C A Bruce, *Dependence of ink jet dynamics on fluid characteristics*. IBM J. Res. Develop., 1976.
[5] Michael T Flanagan, *Sucrose Class: Some Physical Properties of Aqueous Sucrose Solutions*. http://www.ee.ucl.ac.uk/˜mflanaga/java/index.html, 2008.
[6] S K Aslanov, *Theory of the breakup of a liquid jet into drops*. Tech. Phys. Journal, v.44 n.11, 1999.
[7] O Breslouer, *Rayleigh-Plateau instability: falling jet*. Princeton University, 2010.
[8] T R Akylas, *Lecture 5: Fluid Jets*. http://web.mit.edu/1.63/www/Lecnotes/Surfacetension/Lecture5.pdf, MIT, 2004.

6. Figures

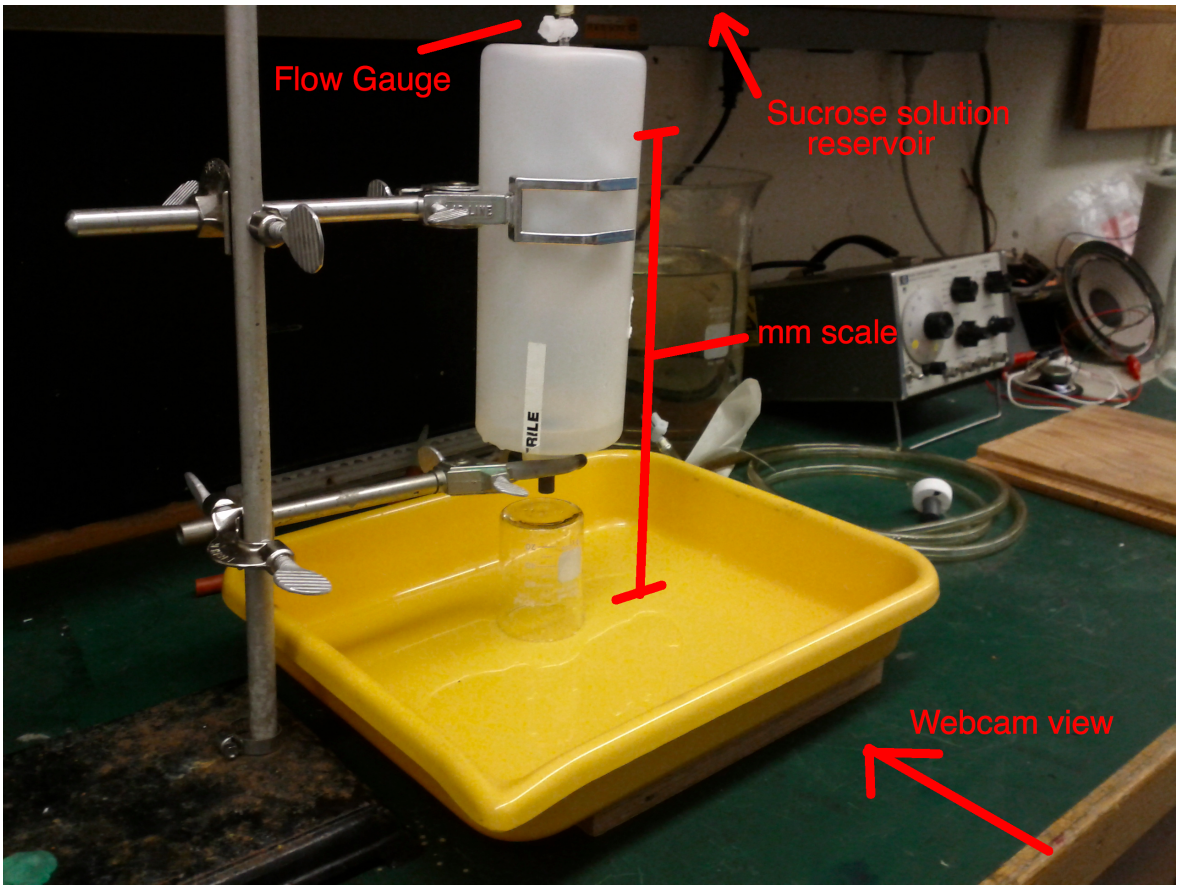

Figure 1. Experimental setup used during data collection.

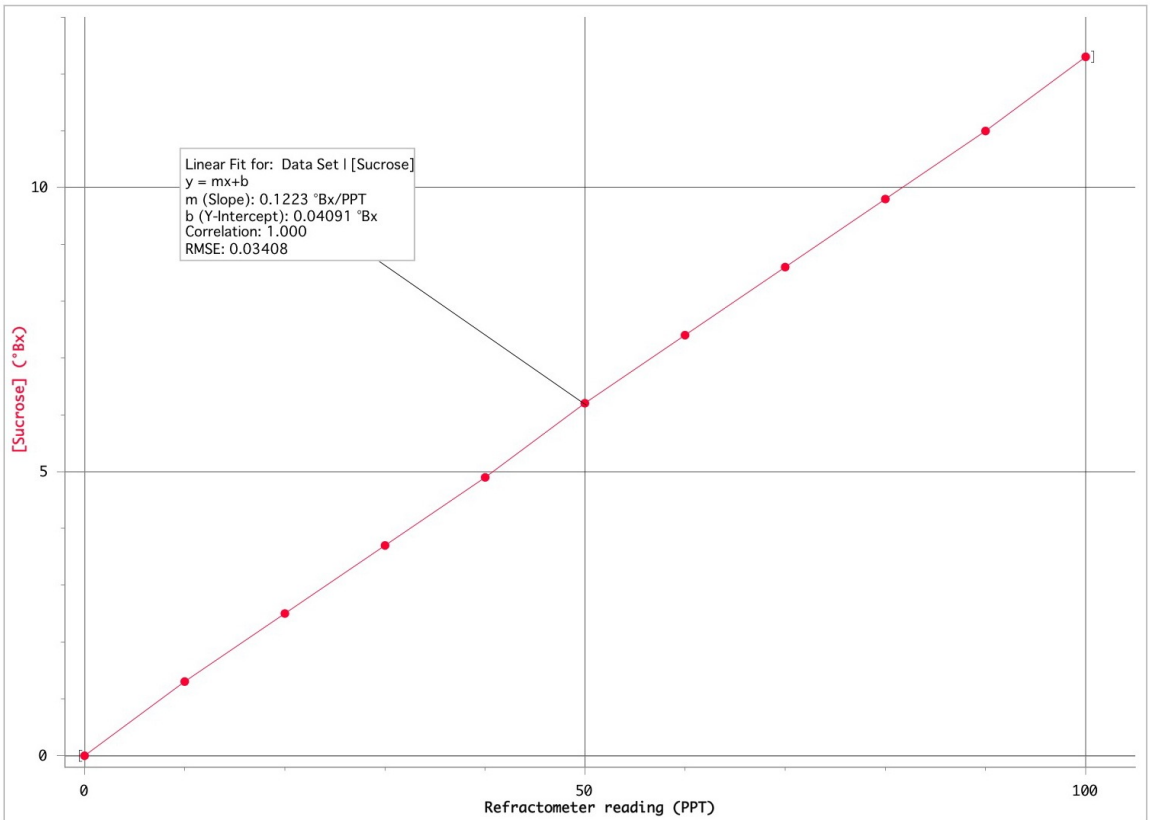

FIGURE 2. Calibration scale used to convert refractometer measurements to degrees Brix, considered approximately equivalent to % by weight of solute in sucrose solution. Data points supplied by refractometer manual.

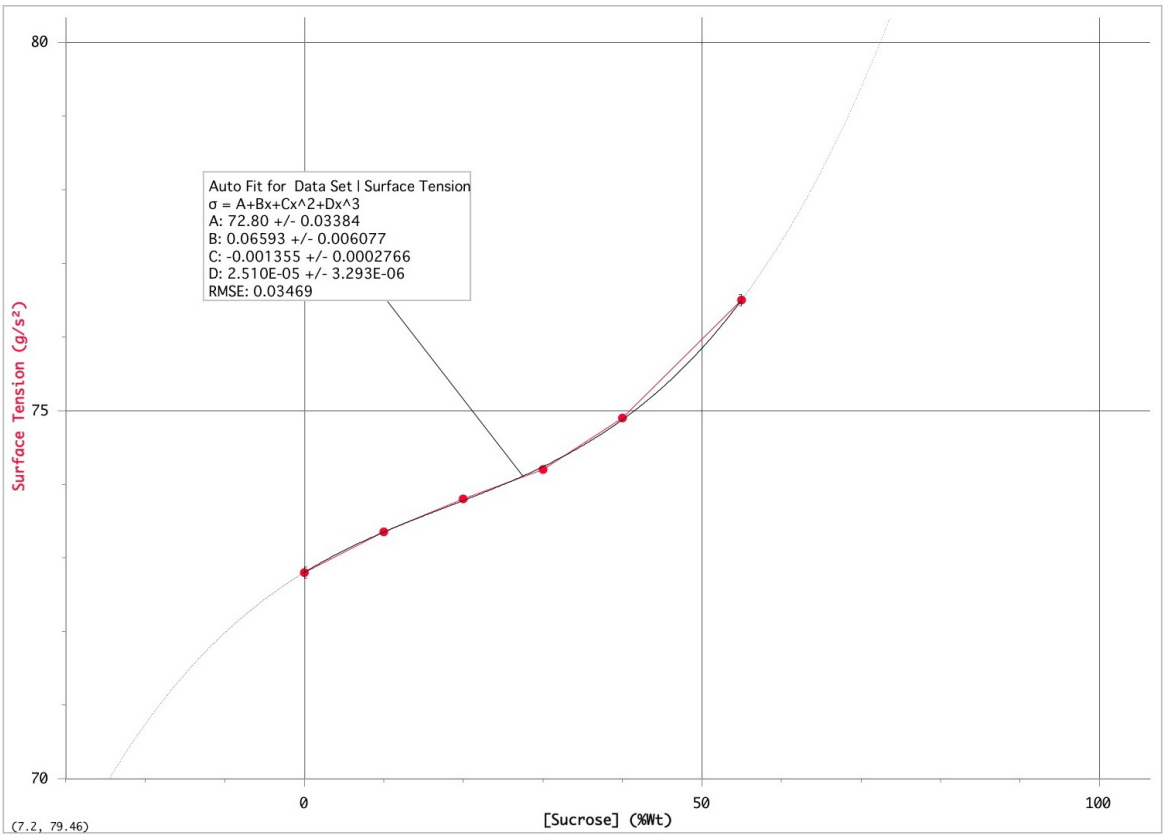

FIGURE 3. Data showing dependence of surface tension in sucrose solution on concentration, along with the polynomial interpolation used for surface tension estimates.

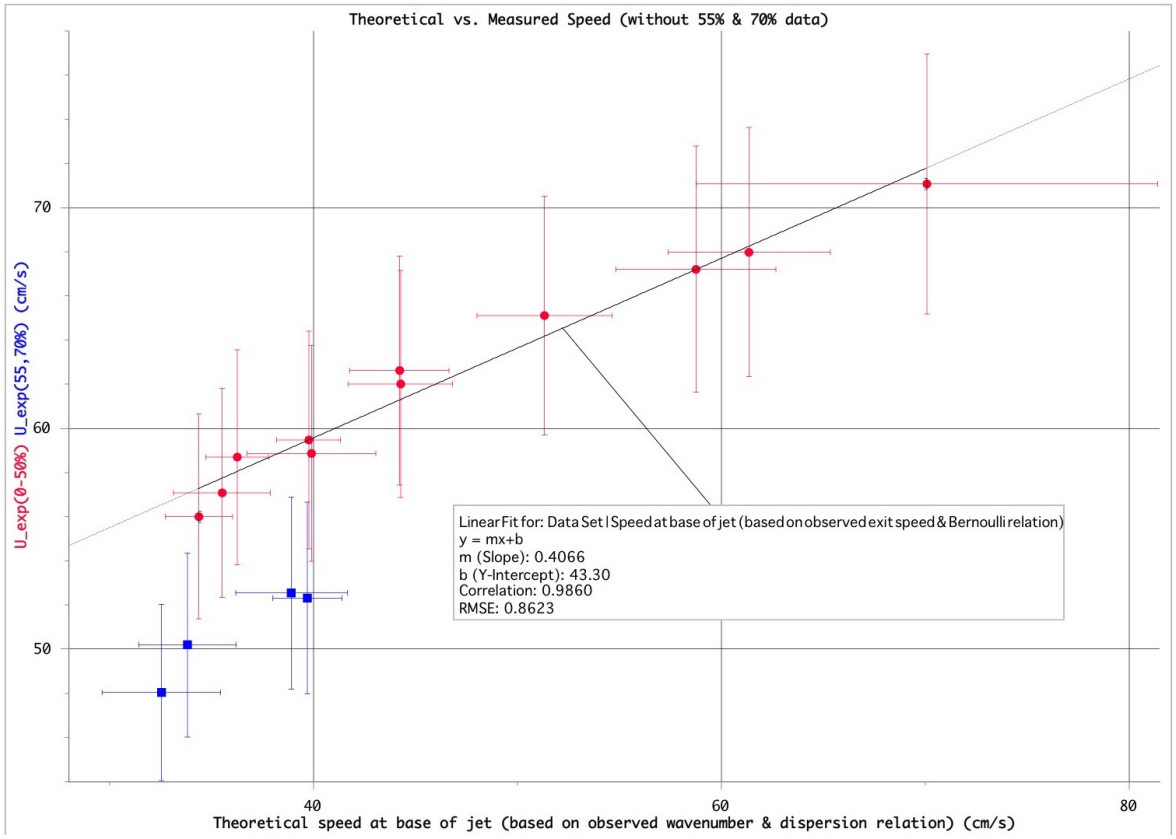

FIGURE 4. Comparison of U_{jet} measurements to values predicted by (5).